IOPscience iopscience.iop.org

Home Search Collections Journals About Contact us My IOPscience

Evidence of a spin liquid with hard-core bosons in a square lattice

This article has been downloaded from IOPscience. Please scroll down to see the full text article.

2012 New J. Phys. 14 113039

(http://iopscience.iop.org/1367-2630/14/11/113039)

View the table of contents for this issue, or go to the journal homepage for more

Download details:
IP Address: 141.211.173.82
The article was downloaded on 25/06/2013 at 20:29

Please note that terms and conditions apply.

New Journal of Physics
The open access journal for physics

Evidence of a spin liquid with hard-core bosons in a square lattice

Y-H Chan[1,2,3] **and L-M Duan**[1,2]

[1] Department of Physics, University of Michigan, Ann Arbor, MI 48109, USA
[2] Center for Quantum Information, IIIS, Tsinghua University, Beijing, China
E-mail: yanghao@umich.edu

New Journal of Physics **14** (2012) 113039 (10pp)
Received 11 September 2012
Published 28 November 2012
Online at http://www.njp.org/
doi:10.1088/1367-2630/14/11/113039

Abstract. We show that laser-assisted hopping of hard-core bosons in a square optical lattice can be described by an antiferromagnetic J_1–J_2 XY model with a tunable ratio of J_2/J_1. We numerically investigated the phase diagram of the J_1–J_2 XY model using both the tensor network algorithm for infinite systems and the exact diagonalization for small clusters and found strong evidence that in the intermediate region around $J_2/J_1 \sim 0.5$, there is a spin liquid phase with vanishing magnetization and valence bond orders, which interconnects the Néel state on the $J_2 \ll J_1$ side and the stripe antiferromagnetic phase on the $J_2 \gg J_1$ side. This finding opens up the possibility of studying the exotic spin liquid phase in a realistic experimental system using ultracold atoms in an optical lattice.

[3] Author to whom any correspondence should be addressed.

Content from this work may be used under the terms of the Creative Commons Attribution-NonCommercial-ShareAlike 3.0 licence. Any further distribution of this work must maintain attribution to the author(s) and the title of the work, journal citation and DOI.

© IOP Publishing Ltd and Deutsche Physikalische Gesellschaft

Contents

1. Introduction

A spin liquid phase is an exotic state of matter that does not break any symmetry of the Hamiltonian and has no conventional order even at zero temperature [1]. A number of microscopic Hamiltonians with frustrated quantum magnetic interaction could support a spin liquid phase [1–7]. In particular, several previous studies done by spin-wave calculation [8], exact diagonalization (ED) [9, 24], series expansions [10, 11] and renormalization group analysis [12, 13] have shown that the antiferromagnetic J_1–J_2 Heisenberg model may have a spin liquid phase in a square lattice. Very recently, large-scale numerical investigations based on complementary methods also found strong evidence supporting this conclusion [4–6]. On the experimental side, several materials are suspected to be in a spin liquid phase at very low temperature [1]. However, due to the complication of physics in these materials, it is hard to make a direct connection between the prediction from the simplified microscopic models and the phenomenology observed in real materials [1]. Ultracold atoms in an optical lattice provide a clean platform to realize microscopic models to allow for a controlled comparison between theory and experiments [14, 15]. Proposals have been made to implement the frustrated magnetic models in an optical lattice [16–18] and various required configurations of the optical lattices have been realized experimentally [17]. However, the direct magnetic Heisenberg coupling, which comes from the higher-order super-exchange interaction, is very weak under typical experimental conditions [16, 19]. It is still very challenging to reach the extremely low temperature required for observing the ground state of the magnetic Heisenberg model in an optical lattice.

In this paper, we show strong evidence that a spin liquid phase can emerge in an antiferromagnetic J_1–J_2 XY model in a square lattice. A previous study with spin-wave calculation has suggested a spin liquid around $J_2/J_1 = 0.5$ [20]. Here, our numerical results confirm this claim and determine the phase boundaries of the model. Our calculations are based on two complementary methods: the recently developed tensor network algorithm applied directly to infinite systems [21, 22] and the ED of small clusters which is combined with the finite-size scaling to infer the phase diagram [23]. Both methods suggest that in a small region around $J_2/J_1 \approx 0.5$, magnetization and valence bond solid orders all vanish, indicating a spin liquid phase as the ground state. Different from a Heisenberg model, an XY model can be realized with hard-core bosons in an optical lattice. In [18], a classical XY model in

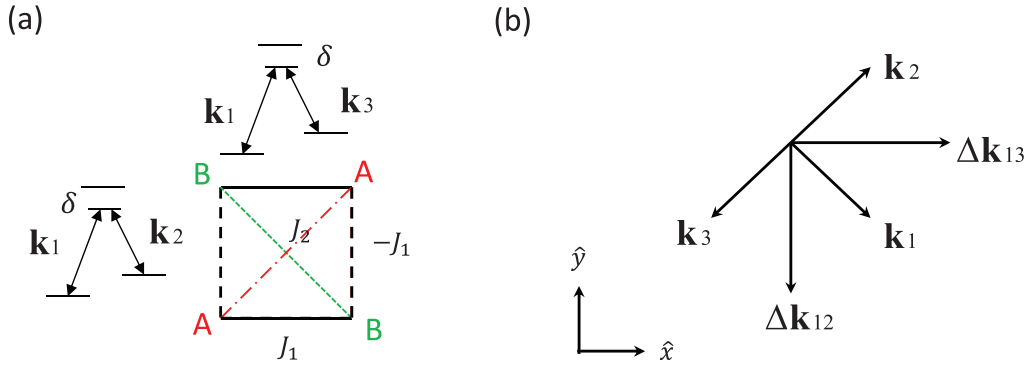

Figure 1. Three Raman laser beams with wave vectors $\mathbf{k_1}$, $\mathbf{k_2}$ and $\mathbf{k_3}$ couple energy levels of A and B sublattices. (a) Hopping in the y-direction is coupled by $\mathbf{k_1}$ and $\mathbf{k_2}$ with strength $-J_1$, while in the x-direction it is coupled by $\mathbf{k_1}$ and $\mathbf{k_3}$ with strength J_1. J_2 is the intrinsic hopping strength in the same sublattice. (b) The configuration of the wave vectors of the three Raman laser beams.

triangular lattices is simulated by confining ultracold bosonic atoms to form two-dimensional (2D) arrays of tubes in which the phase of a superfluid can be described as a classical spin. Our goal is to pursue a quantum XY model. To this purpose, we use local boson occupancy in the optical lattice as pseudo-spins with occupied sites as up spins and empty sites as down spins. Through the control of the laser-assisted hopping in a square lattice [25], we propose a scheme to implement the effective antiferromagnetic couplings for both the neighboring and the next-neighboring sites with a tunable ratio of J_2/J_1. In this implementation, both J_2 and J_1 are determined by the hopping rates of the hard-core bosons in an optical lattice, which is much larger than the conventional super-exchange interaction for ultracold atoms in the Heisenberg model [16, 19]. The large J_1–J_2 couplings open up the possibility to experimentally realize this model and observe its spin liquid phase based on the state-of-the-art technology.

2. Implementation of the J_1–J_2 XY model

The J_1–J_2 XY model is represented by the Hamiltonian

$$H = J_1 \sum_{\langle i,j\rangle} (X_i X_j + Y_i Y_j) + J_2 \sum_{\langle\langle i,j\rangle\rangle} (X_i X_j + Y_i Y_j), \tag{1}$$

where X, Y represent the Pauli operators σ_x and σ_y, $\langle i, j\rangle$ and $\langle\langle i, j\rangle\rangle$ denote, respectively, the neighboring and the next-neighboring sites in a square lattice as shown in figure 1(a). To realize this model with hard-core bosons, we consider ultracold atoms in different hyperfine spins $|a\rangle$ and $|b\rangle$ loaded into alternating square lattices A and B as shown in figure 1(a). This configuration can be experimentally realized with the spin-dependent lattice potential [26]. Atoms in spins $|a\rangle$ (or $|b\rangle$) freely tunnel in the lattice A (or B) with the hopping rate t; however, a direct hopping between the A, B lattices is forbidden due to the spin-dependent potential shift. Instead, the inter-lattice hopping is introduced by the laser-induced Raman transition as shown in figure 1(a). We use three Raman beams, with wave vectors $\mathbf{k}_1$, $\mathbf{k}_2$ and $\mathbf{k}_3$ and Rabi frequencies

$\mathbf{\Omega}_1$, $\mathbf{\Omega}_2$ and $\mathbf{\Omega}_3$, respectively. The directions of the laser beams are shown in figure 1(b) with $\Delta\mathbf{k}_{12} = \mathbf{k}_1 - \mathbf{k}_2 = k_\Delta \hat{y}$ and $\Delta\mathbf{k}_{13} = \mathbf{k}_1 - \mathbf{k}_3 = k_\Delta \hat{x}$. The laser-induced inter-lattice hopping rates for the neighboring sites are then given by $t_x = \int w^*(x_i, y_i)\mathbf{\Omega}_1^*\mathbf{\Omega}_3/\delta\, \mathrm{e}^{\mathrm{i}k\Delta x} w(x_{i+1}, y_i)\mathrm{d}x\, \mathrm{d}y$, and $t_y = \int w^*(x_i, y_i)\mathbf{\Omega}_1^*\mathbf{\Omega}_2/\delta\, \mathrm{e}^{\mathrm{i}k\Delta y} w(x_i, y_{i+1})\mathrm{d}x\, \mathrm{d}y$, for the hopping along the x, y directions, respectively, where δ is the detuning. Assume that $\mathbf{\Omega}_3 = -\mathbf{\Omega}_2$ and the Wannier function $w(x_i, y_i)$ symmetric along the x, y directions, we have $t_x = -t_y = t'$ (we can always choose $t' > 0$ by setting an appropriate relative phase between $\mathbf{\Omega}_1$ and $\mathbf{\Omega}_3$). If the on-site atomic repulsion U satisfies $U \gg t, t'$, we have the hard-core constraint with at most one boson per site. The hard-core bosons in this square lattice are then described by the Hamiltonian

$$H = t' \sum_{\langle i,j\rangle_x} a_i^\dagger b_j - t' \sum_{\langle i,j\rangle_y} a_i^\dagger b_j - t \sum_{\langle\langle i,j\rangle\rangle} (a_i^\dagger a_j + b_i^\dagger b_j) + \mathrm{h.c.} \tag{2}$$

The hard-core bosons a_i, b_j satisfy the same commutators as the Pauli operators σ_i^-, σ_j^-, so with the mapping $a_i \to \sigma_i^-$ and $b_j \to \sigma_j^-$ for the odd numbers of rows, and $a_i \to -\sigma_i^-$ and $b_j \to -\sigma_j^-$ for the even numbers of rows, the Hamiltonian (2) is mapped to the J_1–J_2 XY model in equation (1) with $J_1 = t'/2 > 0$ and $J_2 = t/2 > 0$. Apparently, the ratio J_2/J_1 is tunable by changing the magnitude of the Rabi frequencies $\mathbf{\Omega}_1^*\mathbf{\Omega}_3$.

3. Numerical simulation

In the following, we calculate the phase diagram of the Hamiltonian (1) as a function of the dimensionless parameter J_2/J_1 (J_1 is taken as the energy unit). We limit our discussion to a half-filling case. In the limit $J_2/J_1 \ll 1$, the J_1 term dominates and the ground state is magnetized with a Néel order at the momentum $k = (\pi, \pi)$. In the opposite limit $J_2/J_1 \gg 1$, the ground state has a stripe magnetic order at the momentum $(\pi, 0)$ or $(0, \pi)$, which minimizes the energy of the J_2 term. In the intermediate region with $J_2/J_1 \sim 0.5$, the Hamiltonian is highly frustrated with competing interaction terms. Our main purpose is to find the phase diagram in this region through controlled numerical simulations.

Our numerical simulations are based on two complementary methods: ED for small clusters [23] and tensor network simulation for infinite systems [21, 22]. The ED method is limited by the cluster size, and we use extrapolation based on the finite-size scaling to infer the phase diagram for the infinite system. The tensor network algorithm is a recently developed simulation method inspired by quantum information theory [21]. It can be considered as an extension of the density matrix renormalization group (DMRG) method to the 2D case, replacing the matrix product state in the DMRG method with the tensor network state that better matches the geometry of the underlying lattice [21]. We use a particular version of the tensor network algorithms, the infinite projected entangled pair states (iPEPS) method [22], which applies directly to infinite systems using the translational symmetry. To take into account the ordered states for the Hamiltonian (1) that spontaneously break the translational symmetry, in our simulation we take a unit cell (typically 2×2 and 4×4) that is large enough to incorporate the relevant symmetry breaking orders [28]. We apply imaginary time evolution to reach the ground state of the Hamiltonian. To avoid being stuck in a metastable state, we take a number of random initial states for the imaginary time evolution and pick the ground state as the one which has the minimum energy over all the trials. The accuracy of the iPEPS simulation depends on the internal dimension D of the tensor network state. The simulation time scales up very rapidly

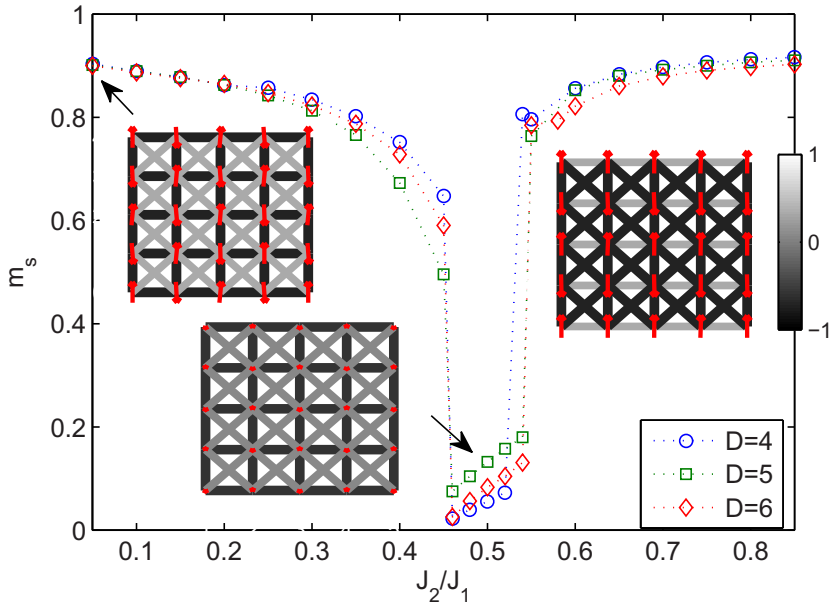

Figure 2. Average magnetization m_s as a function of J_2/J_1. The insets show the spin configuration and the valence bond distribution $\langle \sigma_i \cdot \sigma_j \rangle$ at $J_2/J_1 = 0$, 0.5 and 0.9 obtained with the iPEPS on a 4×4 unit cell with $D = 6$. The width and color of the bonds are scaled such that the negative energy is shown by a thicker bond with a darker color and the positive energy is shown by a thinner bond with a lighter color and the length of the spin is proportional to its magnetic moment m_s.

with the dimension D, which limits D to a small value in practice. We typically take D between 4 and 6 in our simulation.

3.1. Local order parameters from infinite projected entangled pair states (iPEPS)

Figure 2 shows the major result from the iPEPS simulation. First, we look at the average magnetization $m_s = (1/N_s) \sum_i \sqrt{X_i^2 + Y_i^2 + Z_i^2}$ as a function of J_2/J_1, where the average is taken over the N_s sites in the unit cell. The calculation shows that for small or large J_2/J_1, the ground states are magnetic (with the Néel or the stripe order, respectively), which is consistent with our intuitive picture. In the intermediate region with $0.46 \leqslant J_2/J_1 \leqslant 0.54$, there is a sudden drop of all the magnetic orders to a tiny value. Although the iPEPS method under a small dimension D could be biased toward a less entangled state, which is typically an ordered state, it would not be biased toward a disordered spin liquid state. So, when we see a sudden large drop of the magnetic orders from the simulation, it must be a real effect, strongly indicating that there is a new phase in the intermediate region with vanishing magnetic orders. The remaining small m_s may be due to the finite dimension D and should vanish when D is scaled up.

To figure out the property of the phase in the intermediate region, we further check different kinds of valence bond solid orders. We calculate all the neighboring valence bonds $\langle \boldsymbol{\sigma}_i \cdot \boldsymbol{\sigma}_j \rangle$ in the unit cell and the result is shown in figure 2. For a valence bond solid state, the spatial symmetry should be spontaneously broken for the valence bond distribution. Figure 2 shows

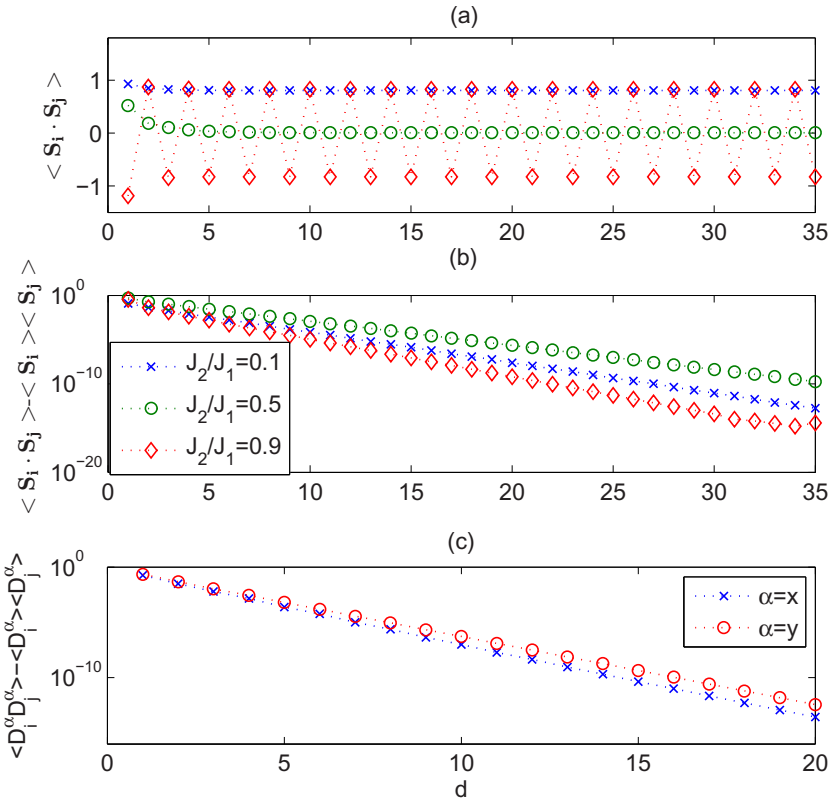

Figure 3. (a) Spin–spin correlation $\langle \sigma_i \cdot \sigma_j \rangle$ as a function of distance d along the diagonal direction at $J_2/J_1 = 0.1$ (cross), 0.5 (circle) and 0.9 (open diamond). (b) Semi-log plot of spin–spin correlation $\langle \Delta\sigma_i \cdot \Delta\sigma_j \rangle$ after subtracting the local averages. (c) Semi-log plot of dimer–dimer correlation $\langle \Delta D_i^\alpha \Delta D_j^\alpha \rangle$ ($\alpha = x, y$) as a function of distance d along the diagonal direction at $J_2/J_1 = 0.5$.

that in the entire region of J_2/J_1, the valence bond distribution has the same symmetry as the underlying Hamiltonian, which indicates that the ground state of the Hamiltonian (1) has no valence bond solid orders. Together with the above calculation of the magnetic orders, this suggests that the Hamiltonian (1) has a spin liquid phase with no orders in the intermediate region with $0.46 \leqslant J_2/J_1 \leqslant 0.54$. This spin liquid phase seems to have the same feature as the $Z2$ spin liquid in the intermediate coupling region of the J_1–J_2 Heisenberg model found in the recent numerical simulation [4, 5].

3.2. Long-range spin–spin and dimer correlations from iPEPS

To further confirm this picture, we calculate the long-range spin correlation and dimer correlation with the iPEPS method and the result is shown in figure 3 for $J_2/J_1 = 0.1, 0.5$ and 0.9. The spin correlation $\langle \sigma_i \cdot \sigma_j \rangle$ is calculated along the diagonal direction $\hat{x} + \hat{y}$. Both the Néel and the stripe phases have long-range correlations, with constant or staggered values along the diagonal direction. The intermediate phase has an exponentially decaying spin–spin correlation, which is in agreement with the behavior of the $Z2$ spin liquid phase with a finite spin gap [1, 4]. The dimer operator D_i^α is defined by $D_i^\alpha = \sigma_i \cdot \sigma_{i+\alpha}$ for the bond $(i, i+\alpha)$,

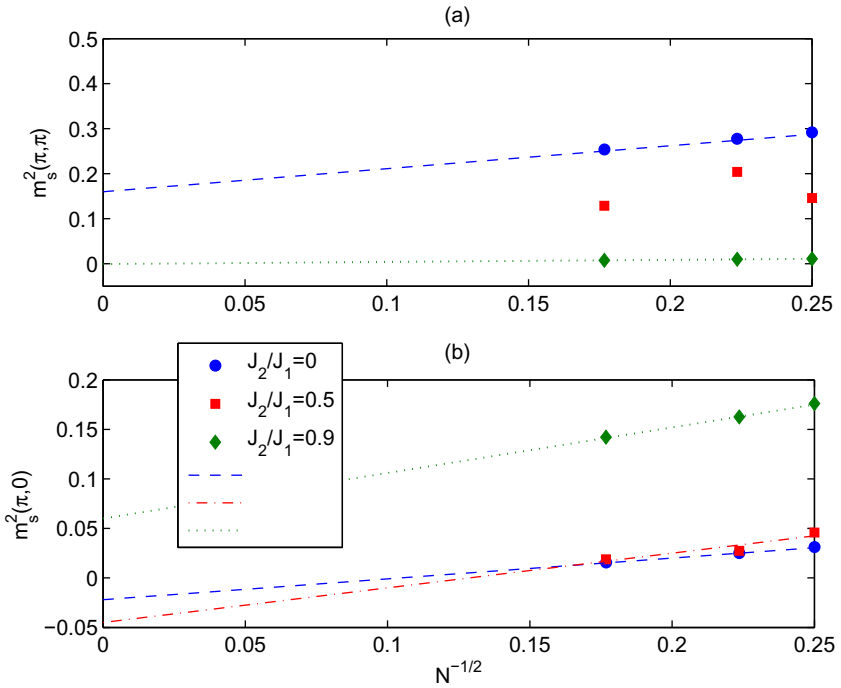

Figure 4. Finite-size scaling of the magnetic order parameter at (a) $\mathbf{k} = (\pi, \pi)$ and (b) $\mathbf{k} = (\pi, 0)$ at $J_2/J_1 = 0$ (dot), 0.5 (square) and 0.9 (diamond).

where $\alpha = \hat{x}$ or $\hat{y}$ denotes the orientation of the dimer. In figure 3(c), we show the dimer–dimer correlations $\langle \Delta D_i^x \Delta D_j^x \rangle$ and $\langle \Delta D_i^y \Delta D_j^y \rangle$ at $J_2/J_1 = 0.5$ along the diagonal direction, where $\Delta D_i \equiv D_i - \langle D_i \rangle$. The correlations decay exponentially with distance, in agreement with a spin liquid phase with no dimer orders.

3.3. Structure factors from the exact diagonalization method

In the following, we present a study of the Hamiltonian (1) with the complementary ED method, which provides further evidence for a spin liquid phase in the intermediate region. To be consistent with the periodic boundary condition required for the finite-size scaling and to incorporate the momentum $k = (\pi, \pi)$ responsible for the Néel order, the size of the clusters for the ED is taken to be 16, 20 and 32 sites[4]. From the spin correlation $\langle \sigma_i \cdot \sigma_j \rangle$, we calculate the corresponding static structure factor $m_s^2(\mathbf{k}, N) = (1/N) \sum_{ij} e^{i\mathbf{k}\cdot(\mathbf{r}_i - \mathbf{r}_j)} \langle \Delta\sigma_i \cdot \Delta\sigma_j \rangle$, where N is the size of the cluster and $\Delta\sigma_i \equiv \sigma_i - \langle \sigma_i \rangle$. The Néel order and the stripe order correspond to peaks at $\mathbf{k} = (\pi, \pi)$ and $(\pi, 0)$, respectively. Finite-size clusters always have non-zero order parameters, and one needs to do finite-size scaling, with a simple scaling formula $m_s^2(\mathbf{k}, N) = m_s^2(\mathbf{k}, \infty) + a/\sqrt{N}$ ($\sqrt{N}$ corresponds to the linear size), to infer the value of $m_s^2(\mathbf{k}, \infty)$ for the infinite system. In figure 4, we show the finite-size scaling for $m_s^2(\mathbf{k}, N)$ at $J_2/J_1 = 0, 0.5$ and 0.9 in three different regions. The results are consistent with the findings of the iPEPS method, i.e. there is a stripe order with $\mathbf{k} = (\pi, 0)$ at $J_2/J_1 = 0.9$ and a Néel order with $\mathbf{k} = (\pi, \pi)$ at $J_2/J_1 = 0$. At $J_2/J_1 = 0.5$, the finite-size scaling indicates a vanishing stripe order. However,

[4] 20 and 32 sites cluster are defined with base side vectors (4,2) and (4,4), respectively.

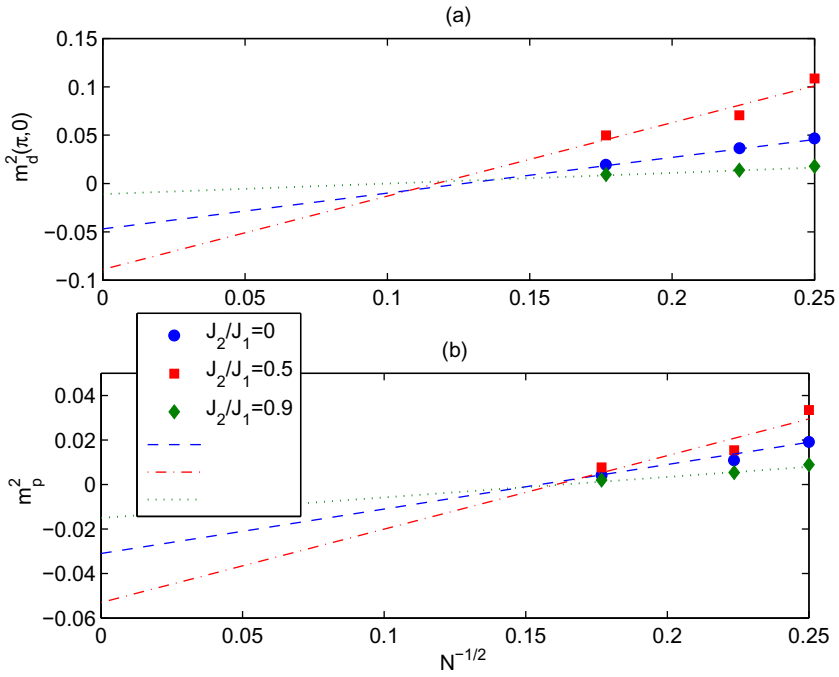

Figure 5. Finite-size scaling of the dimer order parameter at $\mathbf{k} = (\pi, 0)$ and the plaquette order parameter at $\mathbf{k} = (\pi, \pi)$ at $J_2/J_1 = 0$ (dot), 0.5 (square) and 0.9 (diamond).

at $\mathbf{k} = (\pi, \pi)$, the data become non-monotonic with N due to the shape of the cluster and the finite-size scaling becomes inconclusive in this case. The non-monotonic shape effect has also been observed in ED for the J_1–J_2 Heisenberg model [23].

To check for possible valence bond solid orders from ED, we similarly calculate the structure factors $m_d^2(\mathbf{k}, N) = (1/N)\sum_{ij} e^{i\mathbf{k}\cdot(\mathbf{r}_i - \mathbf{r}_j)}\langle \Delta D_i^x \Delta D_j^x \rangle$ and $m_p^2(\mathbf{k}, N) = (1/N)\sum_{ij} e^{i\mathbf{k}\cdot(\mathbf{r}_i - \mathbf{r}_j)}(\langle P_i P_j \rangle$, corresponding respectively to the dimer order D_i^x and the plaquette order $P_i = (Q_i + Q_i^{-1})/2$, where Q_i (Q_i^{-1}) is the clockwise (counterclockwise) cyclic permutation operator on the plaquette i with its explicit (lengthy) expression given in [28, 29]. The rotational symmetry is always preserved at finite size, so we only need to check one component of the dimer order, say D_i^x. At finite size, the structure factors peak at $\mathbf{k} = (\pi, 0)$ for the dimer order D_i^x and at $\mathbf{k} = (\pi, \pi)$ for the plaquette order P_i; however, an extrapolation to the infinite system at these momenta as shown in figure 5 indicates vanishing dimer and plaquette orders in all three regions of J_2/J_1. This result, again, is in agreement with the finding from the iPEPS calculation.

4. Experiment features and setup consideration

Before concluding the paper, we briefly discuss the experimental signature of the three different phases for the Hamiltonian (1) in the implementation with hard-core bosons. The Néel ordered state and the stripe phase correspond to Bose–Einstein condensates at the momenta $\mathbf{k} = (\pi, \pi)$ and $\mathbf{k} = (\pi, 0)$, respectively. The standard time-of-flight imaging measurement can then reveal the condensate peak at these non-trivial momentum points [15]. The spin liquid phase, on

the other hand, would not show any condensation peaks due to a lack of magnetic orders. Furthermore, the exponential decayed spin–spin correlation ensures a spin gap [4, 5], which implies a charge gap in implementation with hard-core bosons. We therefore expect to see an incompressible phase at half-filling, which is different from the Mott insulator state appearing at the integer filling and a charge density wave state with a density order that breaks the translational symmetry. To have some idea of the relevant energy scale, we take an explicit parameter estimation using ^{23}Na atoms as an example. For ^{23}Na atoms in an optical lattice with the laser wave length $\lambda = 594.71\,\text{nm}$ and the recoil energy $E_R = 24.4\,\text{kHz}$ [27], we find that J_2 in the Hamiltonian (1) is about $J_2 \sim 500\,\text{Hz}$ when the lattice depth $V_0 = 10\ E_R$. The laser-induced tunneling J_1 can be easily tuned to be comparable with J_2 by choosing an appropriate intensity for the Raman laser beams. This energy scale is significantly larger compared with the conventional super-exchange energy scale J^2/U. It is hard to calculate the explicit temperature required for the observation of the spin liquid state. However, as the effective interaction rate increases by a factor of U/J, we expect that the required temperature will increases by the same factor U/J compared with the implementation based on the super-exchange interaction. In a real experiment, there is also inhomogeneousity due to a weak global harmonic trap. The spin liquid state corresponds to the half-filling region. The radius of this region can be roughly estimated by $R_{\text{hf}} = \sqrt{(2\Delta_T)/M\omega^2}$, where Δ_T is the triplet spin gap corresponding to the energy required to break a singlet pair, M is the atomic mass and ω is the trapping frequency. The triplet spin gap Δ_T is roughly of the order of J_2 [4]. For ^{23}Na atoms in a trap with the trapping frequency $\omega = 2\pi \times 50\,\text{Hz}$, we estimate $R_{\text{hf}} \sim 44$ lattice sites, which can be resolved easily with the current technology.

5. Conclusion

We have proposed an experimentally feasible scheme to implement the J_1–J_2 XY model with ultracold hard-core bosons in a square optical lattice. Through a detailed numerical simulation of this model using two complementary methods, we found strong evidence that this model has a spin liquid phase in the intermediate region of J_2/J_1. The proposed experimental implementation, with a tunable ratio of J_2/J_1, opens up a realistic possibility of looking for the long-pursued spin liquid phase in a well-controlled Hamiltonian model.

Acknowledgments

We thank Hsiang-Hsuan Hung and Hong-Chen Jiang for helpful discussion. This work was supported by the NBRPC (973 Program) 2011CBA00300 (2011CBA00302), the DARPA OLE program, the IARPA MUSIQC program, the ARO and the AFOSR MURI program.

References

[1] Balents L 2010 *Nature* **464** 199
[2] Meng Z, Lang T, Wessel S, Assaad F and Muramatsu A 2010 *Nature* **464** 847
[3] Yan S, Huse D and White S 2011 *Science* **332** 1173
[4] Jiang H-C, Yao H and Balents L 2012 *Phys. Rev.* B **86** 024424
[5] Wang L, Gu Z-C, Wen X-G and Verstraete F 2011 arXiv:1112.3331
[6] Mezzacapo F 2012 *Phys. Rev.* B **86** 045115

[7] Varney C N, Sun K, Galitski V and Rigol M 2011 *Phys. Rev. Lett.* **107** 077201
[8] Chandra P and Douçot B 1988 *Phys. Rev.* B **38** 9335
[9] Dagotto E and Moreo A 1989 *Phys. Rev.* B **39** 4744
[10] Singh R R P 1989 *Phys. Rev.* B **39** 9760
[11] Singh R R P and Huse D 1989 *Phys. Rev.* B **40** 7247
[12] Einarsson T and Johannesson H 1991 *Phys. Rev.* B **43** 5867
[13] Ferrer J 1993 *Phys. Rev.* B **47** 8769
[14] Jaksch D and Zoller P 2005 *Ann. Phys.* **315** 52
[15] Bloch I, Dalibard J and Zwerger W 2008 *Rev. Mod. Phys.* **80** 885
[16] Duan L-M, Demler E and Lukin M D 2003 *Phys. Rev. Lett.* **91** 090402
[17] Simon J *et al* 2011 *Nature* **472** 307
[18] Struck J *et al* 2011 *Science* **333** 996–9
[19] Foelling S *et al* 2007 *Nature* **448** 1029
[20] Simon P 1997 *Phys. Rev.* B **56** 10975
[21] Verstraete F, Cirac J I and Murg V 2008 *Adv. Phys.* **57** 143
[22] Jordan J *et al* 2008 *Phys. Rev. Lett.* **101** 250602
Jiang H C, Weng Z Y and Xiang T 2008 *Phys. Rev. Lett.* **101** 090603
[23] Capriotti L, Becca F, Parola A and Sorella S 2003 *Phys. Rev.* B **67** 212402
[24] Schulz H J, Ziman T A L and Poilblanc D 1996 *J. Phys.* I **6** 675
[25] Jaksch D and Zoller P 2003 *New J. Phys.* **5** 56
Gerbier F and Dalibard J 2010 *New J. Phys.* **12** 033007
Alba E, Fernandez-Gonzalvo X, Mur-Petit J, Pachos J K and Garcia-Ripoll J J 2011 *Phys. Rev. Lett.* **107** 235301
Aidelsburger M *et al* 2011 arXiv:1110.5314
[26] Mandel O *et al* 2003 *Nature* **425** 937
[27] Xu K *et al* 2005 *Phys. Rev.* A **72** 043604
[28] Chan Y-H, Han Y-J and Duan L-M 2011 *Phys. Rev.* B **84** 224407
[29] Fouet J B, Mambrini M, Sindzingre P and Lhuillier C 2003 *Phys. Rev.* B **67** 054411